

## MODELING OF FLUID INTRUSION INTO POROUS MEDIA WITH MIXED WETTABILITIES USING PORE-NETWORK

Junichiro Takeuchi, Wataru Sumii and Masayuki Fujihara

Graduate School of Agriculture, Kyoto University, Japan

**ABSTRACT:** Water or air intrusion into a porous medium filled with the other fluid is affected by many factors such as size, configuration, and connectivity of pores as well as the contact angle of grain. To deal with these pore-scale factors, a pore-network model is utilized. According to the modified Delaunay method, pore-networks are extracted from randomly packed spherical grains computed by the distinct element method. Displacement processes of two immiscible fluid in a porous medium with mixed wettabilities, are modeled in an invasion percolation manner, in which simultaneous invasion is allowed, and water retention curves in drainage and imbibition processes are computed. The results obtained show that hydrophobic grains do not have just a strong effect on the water retention properties, but also the amount of water/air residue after a drainage/imbibition process depends on the invasion rate.

*Keywords: Water Retention Curve, Residual Water, Trapped Air, Invasion Percolation*

### 1. INTRODUCTION

Soil is an essential medium for plants and animals, because it does not only supports primary producers physically, but is also a supply source of water and nutrients through its pores. So, a large amount of works have involved figuring out the mechanism of soil properties such as the permeability and the water retention properties. While such hydraulic properties of porous media are macroscopic, they originate from microscopic structures such as pore size, configuration, connectivity, and wettability as well as fluid physical properties. Further, the fact that the constitutive relation depends on the history of fluid distribution and the direction of fluid movement complicates matters. One of the methodologies that estimate soil's properties is based on the pore-network model, which treats a pore space in a porous medium as an assemblage of pore segments and incorporates pore-level mechanisms like capillary phenomena. Since the network model for porous media was firstly proposed by Fatt [1], the pore-network approach has been applied in many disciplines, such as the petroleum engineering [2]-[4], the hydrology and soil physics [5]-[9]. Through a series of works, the structure and generation methods of pore-networks, and the algorithms for transport of fluids have evolved by new findings and the development of high-spec apparatuses [10]-[12].

Fatt [1] was the first to utilize a two-dimensional regular cubic network of cylindrical tubes joining at volumeless junctions. After Mohanty and Salter [2] introduced, a pore-network comprised of relatively large pore bodies connected by narrower pore throats are generally

utilized up to the present. The topology of a network can also be represented by a regular two- or three-dimensional lattice, in which sites (pore bodies) have a common coordinate number, which is the number of bonds (pore throats) connected to the site. But real porous media have more irregular structures regarding the coordinate number, pore size, and bond length. And so, several network extraction methods from pixelated images of pores and grains by X-ray tomography or a randomly packed spheres that are simulated by numerical models such as the discrete element method (DEM) have been developed [11], [12].

Percolation theory, which is a branch of probability theory dealing with properties of a network [7], is used to analyze the connectivity of a network when sites or bonds have two different states: 'open' or 'close', with a certain probability. For two-phase immiscible displacements governed by capillary effects in a pore-network, a special version of the percolation theory known as the invasion percolation is often applied [6]-[9]. The invasion percolation originally proposed by Wilkinson and Willemsen [3] is a dynamic percolation process, and accessibility rule is imposed for movement of interfaces between invading and defending fluids. Accessibility to an outside fluid reservoir through sites or bonds filled by the same kind fluid is required to both invading and defending fluids, or to either fluid, depending on the materials and situations of interest.

Water-repellent soils, which have resistance to spontaneous water intrusion, have been reported from the early 1900's in various countries such as New Zealand, Australia, and Netherlands [13]. Many works revealed that hydrophobic grains mixed into normal (hydrophilic) grains have

potential to change the hydraulic properties drastically [14], [15]. Ustohal et al. [15] proposed a functional model to predict the hydraulic properties of porous media variously mixed with hydrophobic grains by stochastically integrating clusters that contain multiple grains, based on the Brooks-Corey model. Takeuchi et al. [16] extended the model by Ustohal et al. [15] and developed a distributed model to estimate the water retention properties. However, in the cluster-based models the influences by hydrophobic grains are blunted when larger clusters are used. Moreover, the distribution of pore sizes, which is essential for estimating the hydraulic properties, must be identified with observed data indirectly or from literature.

The objective of this study is to develop a pore-network model for predicting the hydraulic properties of porous media mixed with hydrophobic grains at various fractions, incorporating pore-level capillary actions. In this paper, changes of water retention properties by mixed hydrophobic grains are investigated, focusing on the algorithm used in the invasion percolation. While invading fluid enters only the most invadable pore in one step in the ordinary invasion percolation, simultaneous invasions are allowed in this study, and the effects are examined through numerical experiments.

## 2. MODEL DESCRIPTION

### 2.1 Generation of Pore-Network Model

In this study, the modified Delaunay-tessellation approach proposed by Al-Raoush et al. [11] is employed to generate pore-networks. Delaunay tessellation is a widely used spatial segmentation method for generation of

computational meshes used in numerical simulations. After a 3-D domain is discretized into tetrahedral subdomains, based on the spherical grain's centers as nodes, a network is generated by connecting inner points of neighboring subdomains. But the network has two significant problems. First, the network has a fixed coordination number, which equals to four since a tetrahedron has four faces. Second, the location and size of pore bodies are not correct. To overcome these problems, a modified approach in which multiple subdomains are merged for identification of pore body's location and size is proposed. A realistic irregular pore-network of randomly packed spherical grains could be obtained by this modification.

Here, virtual porous media randomly packed with equally-sized spherical grains are produced by DEM. To obtain relatively dense porous media, a small value was given to the friction coefficient in this study. About 58 hundreds grains are packed in a cuboidal container as shown in Fig. 1 (a). The length of horizontal edge corresponds to the length of 16 straightly lined grains, and the size of a network is derived from the required minimum network size [6]. The extracted pore-network is also shown in Fig. 1 (b), and the pore-network consists of 14,522 pore bodies and 36,761 pore throats. The spheres in Fig. 1 (b) represent pore bodies, and the pipes connecting pore bodies are pore throats. The shape of a pore throat cross-section is given as the void surrounded by grains as shown in Fig. 2, in which cases of three and four grains are illustrated.

Figure 3 shows the distributions of the coordinate number, the radii of pore body and throat, and the length of pore throat in the extracted pore-network. The radius of a pore throat

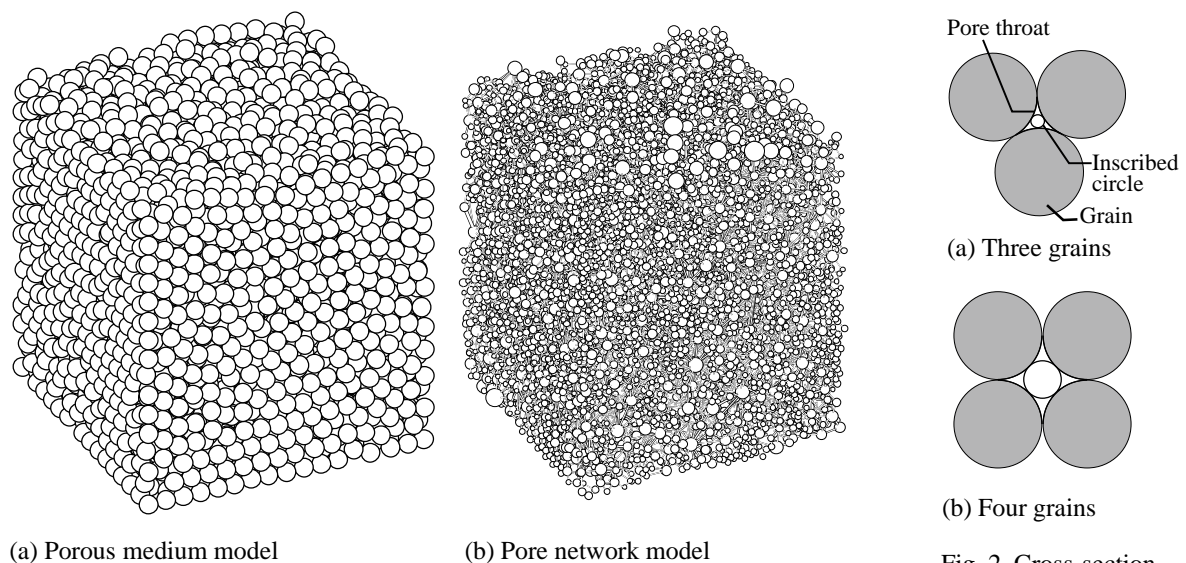


Fig. 2 Cross-section of pore throat

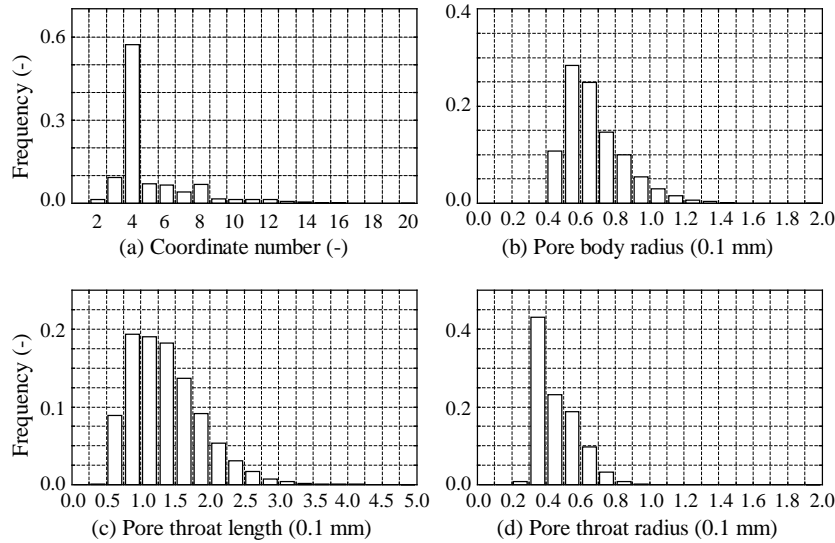


Fig. 3 Histograms of coordinate number and pore sizes

is represented as that of the maximum inscribed circle locating inside the void surrounded by grains as illustrated in Fig. 2. The radius of a pore body is also represented as that of the maximum inscribed sphere locating inside the void in the same way. The length of a pore throat represents the length between the centers of pore bodies connected by the pore throat.

Figure 4 shows the correlations of the coordinate number and pore body size between pore bodies connected by a throat. The graphs in both figures are almost flat, and this means that there is no spatial correlation in the coordinate number and the size between pore bodies.

## 2.2 Pore-Level Description

In this study, it is assumed that one fluid displaces the other fluid at a sufficiently low capillary number. So, the movement of an interface between two immiscible fluids occurs quasi-statically by capillary forces. In addition, only piston-like displacements are assumed in both drainage and imbibition processes. According to Dullien et al. [17], water residue in a porous medium packed with glass beads with smooth surface was approximately 10% after a drainage process, while that in a medium with roughened glass beads by etching was approximately 1%. This result indicates that the effects of wetting layers and films are negligible when smooth glass beads are used.

Furthermore, neither residue in a drainage process nor pre-invasion in an imbibition process along the corners of hydrophilic pore throats and bodies by wetting fluid are considered in this study. Accordingly, pendular rings of wetting fluid around the two grains contact are not considered in

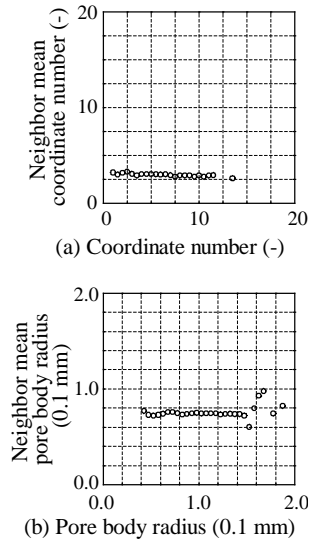


Fig. 4 Correlation of neighbor pore body

this model.

Pores, which represents both of pore bodies and throats here, have two states: 'Water' and 'Air'. The Water/Air state represents the pore is filled with water/air. Therefore, the meniscus is formed on a boundary of a pore body in one state and a neighbor pore throat in the other state. Whether one fluid can intrude into the other fluid or not depends on the magnitude relationship between the capillary pressure  $P_c$  on the interface and the capillary entry pressure  $P_e$  assigned to all pores. These are given by the following equations.

$$P_c = P_a - P_w \quad (1)$$

$$P_e = \frac{\sigma \cos \varphi_e}{R} \quad (2)$$

where  $P_a$  and  $P_w$  are the air and water pressures at the vicinity of the interface, respectively,  $\sigma$  is the interfacial tension,  $\varphi_e$  is the equivalent contact angle of the pore, and  $R (= A / L)$  is the hydraulic radius,  $A$  is the cross-section area of the pore, and  $L$  is the perimeter of the pore cross-section. In this study, a pore body are represented as a sphere, which is the maximum inscribed sphere in the void surrounded by multiple grains as described in the subsection of 'Generation of Pore-Network Model'. A pore throat is represented by a tube with constant cross-section, and the shape of the cross-section is represented as a grain boundary void, which has more than three cusps, as illustrated in Fig. 2.

The equivalent contact angle  $\varphi_e$  of a pore is assumed to be given by the Cassie-Baxter equation. When the pore is composed of multiple grains with two types of wettability, the equivalent contact angle is described as follows.

$$\cos \varphi_e = \frac{N_1}{N_1 + N_2} \cos \varphi_1 + \frac{N_2}{N_1 + N_2} \cos \varphi_2 \quad (3)$$

where  $N_1$  and  $N_2$  are the numbers of hydrophilic and hydrophobic grains surrounding the pore, respectively; and  $\varphi_1$  and  $\varphi_2$  are the contact angles of hydrophilic and hydrophobic grains, respectively.

In addition to these equations, invadability  $I$ , which is an index that represents the degree of easiness when one fluid invades a pore filled with the other fluid, is defined as follows.

$$I = P_c - P_e \quad (4)$$

In a drainage process, invading fluid (air) can intrude into a pore, only when the invadability is positive. On the other hand, invading fluid (water) can intrude in an imbibition process, only when the invadability is negative.

### 2.3 Generalized Invasion Percolation

Two types of boundary are given to the pore-network: one is a no-flow boundary, and the other is an open-flow boundary. A sufficiently large reservoir which is a supply source or sink is connected to the open-flow boundary. In this study, the no-flow boundary is given to the four lateral faces, and the open-flow boundary to the top and bottom faces. The top face contacts with an air reservoir, and the bottom with a water reservoir. The air pressure inside and outside of the pore-network is set as a constant, and the water pressure inside of the pore-network is determined by the pressure imposed on the bottom, assuming the hydrostatic pressure.

Drainage and imbibition processes are described in an invasion-percolation manner. In the invasion percolation, fluids are required to satisfy an accessibility rule in addition to the invadability condition. In this study, the accessibility rule is imposed to both invading and defending fluids to connect to each other's reservoir through pores filled with the same fluid,

when the interface moves. The algorithm of the invasion percolation for computation of one sample in a drainage process is described as follows:

1. All the pore bodies and throats are filled with water, and a certain water pressure is imposed on the bottom of the pore-network.
2. Produce a list of all the pore bodies and throats which are defending against air intrusion and satisfy the accessibility rule, and sort these in descending order based on the invadability value.
3. Among the listed pore bodies and throats, the interfaces of the top  $N^{IP}$  in the list are moved simultaneously (the state in the pores is changed from Water to Air) if the invadability value is positive.
4. Iterate the processes 2 and 3 until no state change occurs, and saturation of the pore-network is calculated when a steady state is achieved.

If the next sample is computed continuously, the obtained result is used as an initial condition and the water pressure imposed on the bottom is decreased in a stepwise manner, and go back to 2. This process corresponds to the suction method and pressure plate method, in which one sample is used continuously under a gradually changing pressure condition. In contrast, in the soil column method, different samples are used for each pressure condition. So, if the soil column method is supposed, go back to 1 and start from the dry condition for the next pressure.

In an ordinary invasion percolation process, invading fluid is allowed to intrude into only one pore that have the largest invadability, i.e.,  $N^{IP} = 1$ . In this study, simultaneous intrusions into multiple pores are allowed, and this type of invasion percolation is termed as a generalized invasion percolation here. The simultaneous intrusions are considered to correspond to a drainage process with relatively large capillary number.

In a case of an imbibition process, the

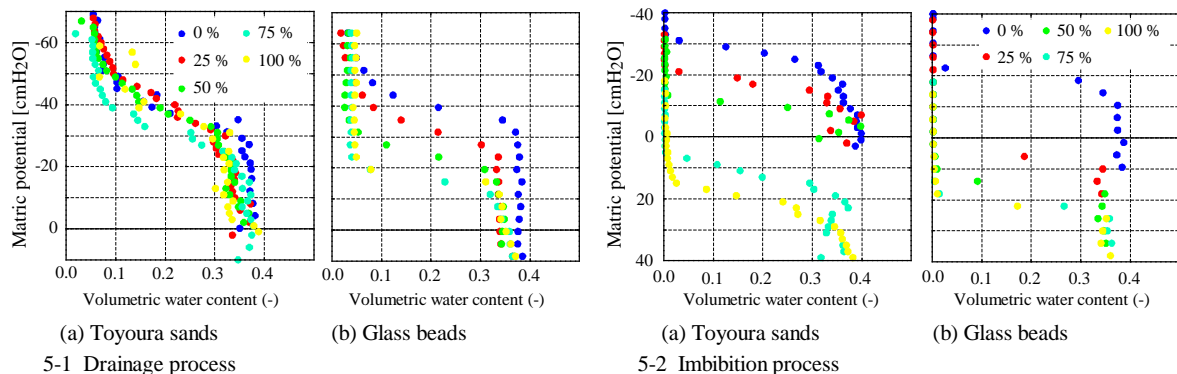


Fig. 5 Measured water retention curves of Toyoura sands and Glass beads

algorithm is described in the same way with the drainage process. The main difference is in the list of candidates. The list in an imbibition process is sorted in an ascending order of the invadability, while it is sorted in a descending order in a drainage process. Then the top  $N^{IP}$  of pores would be invaded by water if the invadability value is negative.

### 3. WATER RETENTION PROPERTIES

#### 3.1 Experimental Results

Toyoura standard sand and glass beads are used as materials. The mean diameter of Toyoura sand is about 0.25 mm, and that of glass beads is 0.2 mm. Toyoura sand and glass beads are hydrophobized by perfluorooctylethyltrichlorosilane ( $(CF_3(CF_2)_7(CH_2)_2 SiCl_3)$ ) and octyltrichlorosilane ( $(CH_3(CH_2)_7SiCl_3)$ ), respectively. Figure 5 shows the measured water retention curves of each material mixed with hydrophobic grains at various mixture fractions by the soil column method [16]. From these figures, it is found that water retention curves are largely altered by the mixed hydrophobic grains, and that the degree of the alteration depends on the mixture fraction.

#### 3.2 Computational Results

Water retention curves are computed using the above mentioned pore-network model in the generalized invasion percolation manner. The contact angles of the hydrophilic and hydrophobic grains are given as 58 degrees and 102 degrees, based on the measurement of the apparent contact angles of glass beads with the sessile drop method [18]. And common values are used for drainage and imbibition processes without considering receding and advancing contact angles. Several options can be considered in the computational

settings about the number of simultaneous intrusions  $N^{IP}$  and the initial condition of each sample. Here two options are given in each setting. Regarding the intrusion number,  $N^{IP}$  is limited to ten in one case, and no limitation is given in the other case. Regarding the initial condition, the previous computed result is given as an initial condition in one case, and the saturated/dry condition is given in a drainage/ imbibition process in the other. Therefore, four cases are considered by the combination of these options. Among these four cases, two cases are shown below: one is the combination of 'limited to ten' and 'previous result', and the other is the combination of 'no limitation' and 'saturated/dry condition'. The former is referred to as Case 1, and the latter as Case 2 in this study. The results of the rest two cases were pretty much the same with Case 1. It is considered that these three cases correspond to a relatively small capillary number, and that Case 2 to a relatively large capillary number.

The computed water retention curves of Case 1 and Case 2 are shown in Fig. 6, and the computed states of pores in the pore-network are shown in Fig. 7, where the black pores represent ones occupied by water and the white pores by air. Figure 6 shows that the water retention curves are altered by hydrophobic grains in common with the experimental results. Some discrepancy is seen especially in the drainage process between the experimental and computational results. While relatively small differences among the various mixture fractions are seen in the experimental results (Fig. 5-1), relatively large differences are seen in the computational results (Fig. 6-1). This suggests that different contact angles, or receding and advancing contact angles, should be used for evaluating the drainage and imbibition processes.

The main difference between Case 1 and Case 2 is seen in residual water in the drainage process

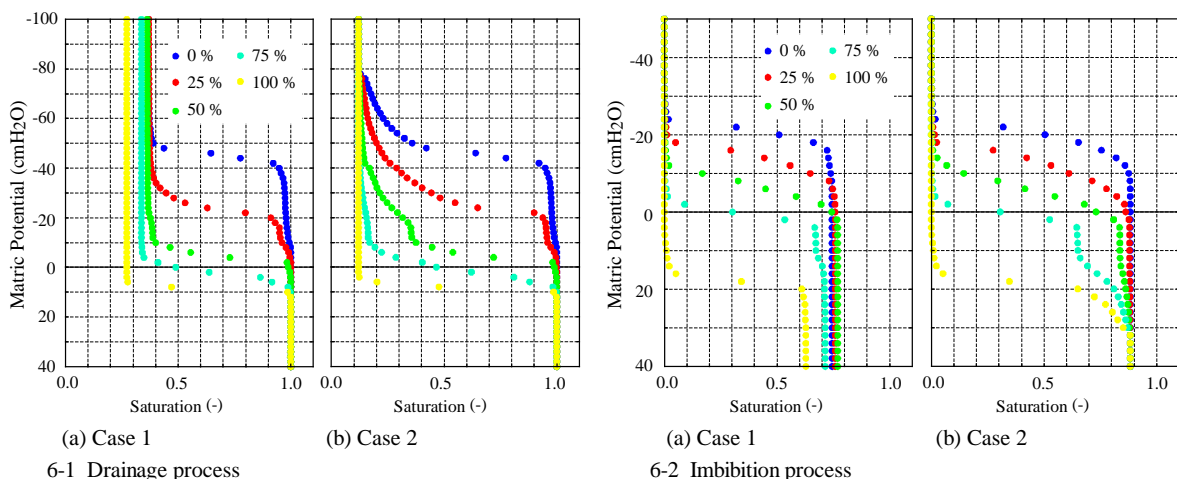
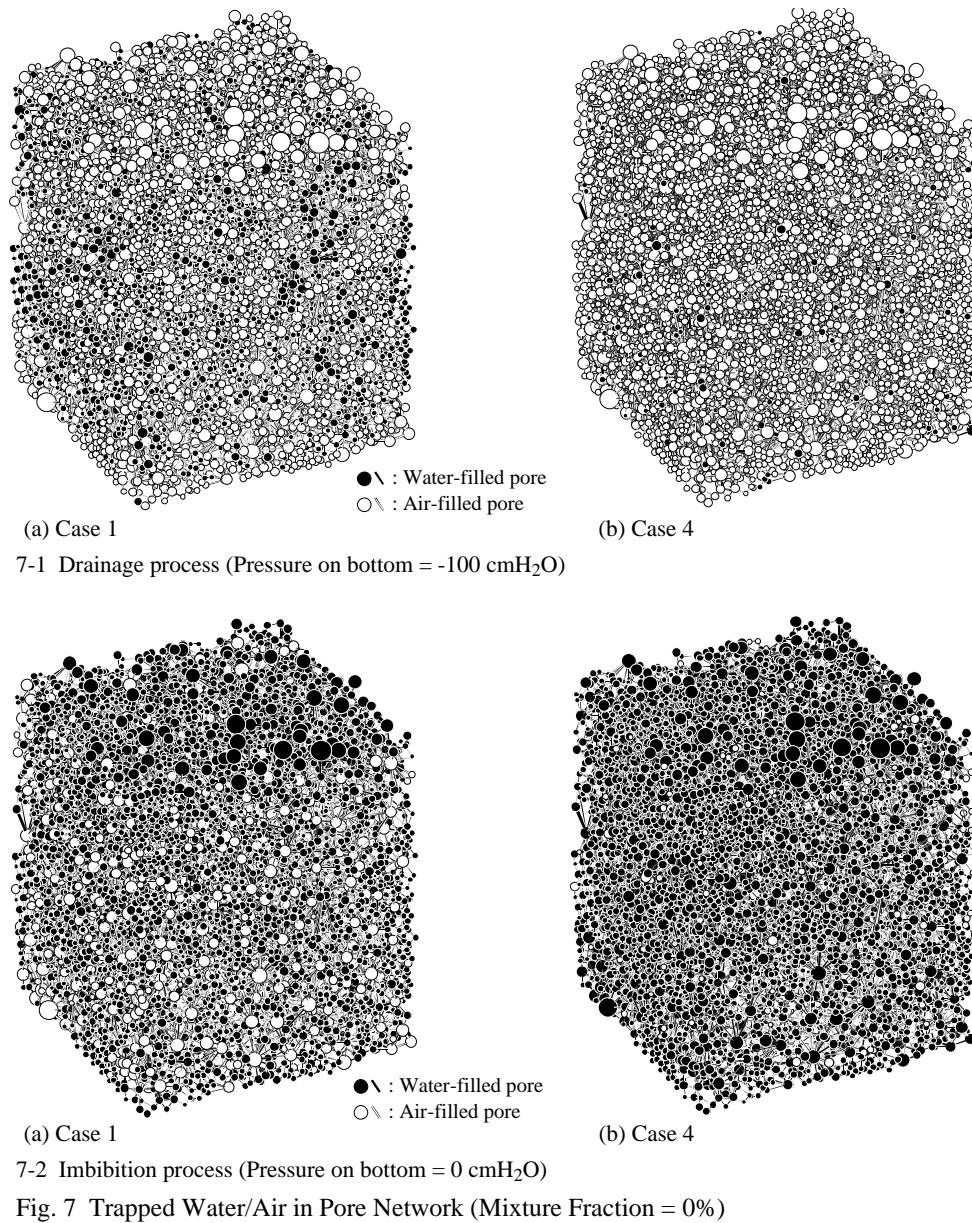


Fig. 6 Computed Water Retention Curves of Case 1 and Case 2





and in trapped air in the imbibition process. While 10% of water or air remains after each process in Case 2, 30% to 40% is left behind in Case 1. From Fig. 7, residual water is seen in clusters of relatively small pore bodies, and trapped air are seen in clusters of relatively large pore bodies in Case 1. In a drainage process, such clusters of smaller pore bodies are formed because water is drained firstly from a sequence of larger pore bodies ahead of smaller ones and the connectivity between the clusters of smaller pore bodies and the outside reservoir is cut off. In the case of the imbibition process, clusters of relatively large pore bodies are formed in the same way.

#### 4. CONCLUSION

Numerical experiments for water retention properties of porous media with mixed wettabilities were conducted, using an extracted pore-network from randomly packed spherical grains. The air/water intrusion process are modeled by the generalized invasion percolation, in which simultaneous intrusions are allowed. Single or a small number of simultaneous intrusions correspond to a relatively small capillary number, and all or a large number of simultaneous intrusions corresponds to a relatively large capillary number. The computational results showed a similarity to the experimental ones in regard to the dependence of the mixture fraction, and that the amount of residual water and trapped air depends on the invasion rate.

## 5. ACKNOWLEDGEMENT

This work was supported by JSPS KAKENHI Grant Number 24780232.

## 6. REFERENCES

- [1] Fatt I, "The network model of porous media", Trans. AIME, Vol. 207, 1956, pp. 144-181.
- [2] Mohanty KK and Salter SJ, "Multiphase flow in porous media: II. Pore-level modeling", SPE 11018 the 57<sup>th</sup> Tech. Conf. at SPE-AIME, New Orleans, Sep., 1982, pp. 26-29.
- [3] Wilkinson D and Willemsen JF, "Invasion percolation: a new form of percolation", J. Phys. A: Math. Gen., Vol. 16, 1983, pp.3365-3376.
- [4] Piri M and Blunt MJ, "Pore-scale modeling of three-phase flow in mixed-wet systems", SPE 77726 the SPE Annual Tech. Conf. and Ex., San Antonio, Texas, Sep., 2002.
- [5] Jerauld GR and Salter SJ, "The effect of pore-structure on hysteresis in relative permeability and capillary pressure: pore-level modeling", Transport in Porous Media, Vol. 5, 1990, pp. 103-151.
- [6] Soll WE and Celia MA, "A modified percolation approach to simulating three-fluid capillary pressure-saturation relationships", Adv. Water Resour., Vol. 16, 1993, pp. 107-126.
- [7] Berkowitz B and Ewing R, "Percolation theory and network modeling applications in soil physics", Surveys in Geophysics, Vol. 19, 1998, pp. 23-72.
- [8] Raoof A and Hassanizadeh SM, "A new formulation for pore-network modeling of two-phase flow", Water Resour. Res., Vol. 48, 2012, W01514, doi: 10.1029/2010WR010180.
- [9] Yang Z, Niemi A, Fagerlund F, and Illangasekare T, "Two-phase flow in rough-walled fractures: comparison of continuum and invasion-percolation models", Water Resour. Res., Vol. 49, 2013, doi: 10.1002/wrcr.20111.
- [10] Blunt MJ, "Flow in porous media – pore-network models and multiphase flow", Current Opinion in Colloid & Interface Science, Vol. 6, 2001, pp. 197-207.
- [11] Al-Raoush R, Thompson K, and Willson CS, "Comparison of network generation technique for unconsolidated porous media", Soil Sci. Soc. Am. J., Vol. 67, 2003, pp. 1687-1700.
- [12] Ngom NF, Garnier P, Monga O, and Peth Stephan, "Extraction of three-dimensional soil pore space from microtomography images using a geometrical approach", Geoderma, Vol. 163, 2011, 127-134.
- [13] DeBano LF, "Water repellency in soils: a historical overview", J. Hydrol., Vol. 231-232, 2000, pp. 4-32.
- [14] Annaka T, "Wettability indices and water characteristics for sands of mixed wettability", J. Jpn. Soc. Soil Phys., Vol. 102, 2006, pp. 79-86.
- [15] Ustohal P, Dtauffer F, and Dracos T. "Measurement and modeling of hydraulic characteristics of unsaturated porous media with mixed wettabilities", J. Contam. Hydrol., Vol. 33, 1998, pp. 5-37.
- [16] Takeuchi J, Takahashi T, and Fujihara M, "Sub-Darcy scale modeling of non-uniform flow through porous media with mixed wettabilities", Int. J. GEOMATE, Vol. 6, 2014, pp. 840-847.
- [17] Dullien FAL, Francis Lai FSY, and Macdonald IF, "Hydraulic continuity of residual wetting phase in porous media", J. Colloid Interface Sci., Vol. 109, 1986, pp. 201-2018.
- [18] Bachmann J, Ellies A, and Hartge KH, "Development and application of a new sessile drop contact angle method to assess soil water repellency", J. Hydrol., Vol. 231-232, 2000, pp. 66-75.

---

*International Journal of GEOMATE, June, 2016, Vol. 10, Issue 22, pp. 1971-1977.*

MS No. 5190 received on June 15, 2015 and reviewed under GEOMATE publication policies. Copyright © 2015, Int. J. of GEOMATE. All rights reserved, including the making of copies unless permission is obtained from the copyright proprietors. Pertinent discussion including authors' closure, if any, will be published in Feb. 2017 if the discussion is received by Aug. 2016.

**Corresponding Author: Junichiro Takeuchi**

---